Published in final edited form as:
Dev Dyn. 2008 May ; 237(5): 1321–1333. doi:10.1002/dvdy.21526.

Retinoic Acid Induces Prostatic Bud Formation

Chad M. Vezina[1], **Sarah H. Allgeier**[2], **Wayne A. Fritz**[1], **Robert W. Moore**[1], **Michael Strerath**[1], **Wade Bushman**[2,3], and **Richard E. Peterson**[1,2,*]

1*University of Wisconsin, School of Pharmacy*

2*University of Wisconsin, Molecular and Environmental Toxicology Center*

3*University of Wisconsin, Department of Surgery, School of Medicine*

Abstract

Formation of prostatic buds from the urogenital sinus (UGS) to initiate prostate development requires localized action of several morphogenetic factors. This report reveals all-*trans*-retinoic acid (RA) to be a powerful inducer of mouse prostatic budding that is associated with reciprocal changes in expression of two regulators of budding: sonic hedgehog (*Shh*) and bone morphogenetic protein 4 (*Bmp4*). Localization of retinoid signaling and expression of RA synthesis, metabolism and receptor genes in the UGS on embryonic days 14.5-17.5 implicate RA in the mechanism of bud initiation. In UGS organ culture, RA increased prostatic budding, increased *Shh* expression, and decreased *Bmp4*. Prostatic budding was stimulated in the absence of RA by recombinant SHH, by blocking BMP4 signaling with NOGGIN, or by combined treatment with SHH and NOGGIN in UGS organ culture media. These observations suggest that reciprocal changes in hedgehog and BMP signaling by RA may regulate bud initiation.

Keywords

Urogenital Sinus; Retinoic Acid; Development; Mouse; Prostate; Bud Formation; SHH; BMP4

INTRODUCTION

The prostate anlage, the urogenital sinus (UGS), is formed on murine embryonic day (E) 13.5 as a simple cylindrical structure comprised of gut-derived endoderm surrounded by mesenchyme. Development of mature prostate from the UGS requires androgen-dependent crosstalk between mesenchyme and epithelium (Cunha and Lung, 1978; Goldstein and Wilson, 1975). Bidirectional crosstalk triggers initiation of solid epithelial buds on E16.5. Prostatic buds emerge in a spatially defined pattern that establishes the position of mature dorsal, lateral, ventral, and anterior prostate lobes (Cunha et al., 1987). Buds that give rise to dorsal and anterior prostate ducts are the first to form in the mouse UGS (E16.5) and lateral and ventral prostatic buds form about one day later (Lin et al., 2003). A finite quantity of prostatic buds are formed in each region of the UGS during *in utero* mouse development: there is an average of 52 dorsal prostate buds, 5-6 anterior buds, 6 lateral buds, and 8 ventral buds (Lin et al., 2003). Most of the prostate buds that form during the initial stage of prostate development continue to elongate and then undergo postnatal branching morphogenesis, canalization and differentiation. Prostate branching morphogenesis nears completion by postnatal day (P) 20 and secretory function is acquired during puberty.

*Correspondence: Dr. Richard E. Peterson, University of Wisconsin, School of Pharmacy, 777 Highland Ave, Madison, WI 53705, Phone (608) 263-5453, Email: repeterson@pharmacy.wisc.edu

Numerous signaling factors have been implicated in growth and homeostasis of the mature prostate and in regulation of early postnatal prostatic branching morphogenesis and cytodifferentiation. However, relatively few signaling pathways have been directly implicated in prostatic bud initiation. Activation of androgen receptors in UGS mesenchyme is critical for prostatic budding (Lasnitzki and Mizuno, 1980). Signaling by fibroblast growth factor 10 (FGF10) has been shown to be essential for budding to occur (Doles et al., 2006; Thomson and Cunha, 1999). Epidermal growth factor (Saito and Mizuno, 1997), homeobox genes (Podlasek et al., 1997; Warot et al., 1997), and both low-dose and high-dose estrogens (vom Saal et al., 1997) have been shown to influence budding, but the mechanisms by which these effects occur is unclear. The bone morphogenetic proteins (BMPs) 4 and 7 (Cook et al., 2007; Grishina et al., 2005) and wingless integration site A (WNT5A; unpublished observations) can directly inhibit bud formation while hedgehog (Hh) signaling has been implicated as a positive regulator of budding (Podlasek et al., 1999, Lamm et al., 2002, Doles et al., 2006). What remains to be determined is how these positive and negative influences are orchestrated to yield the reproducible pattern and quantity of buds that form on select surfaces of the male mouse UGS during fetal development.

We hypothesized that retinoic acid may also play a role in regulating prostatic budding. Retinoids are essential regulators of organogenesis, but their role in prostatic budding has not been determined. All-*trans*-retinoic acid (RA) is a biologically active form of vitamin A and its synthesis and metabolism is carefully regulated in a temporally- and spatially-restricted fashion throughout embryonic development (Clagett-Dame and DeLuca, 2002). RA is synthesized from vitamin A in a two step oxidation process catalyzed by alcohol and aldehyde dehydrogenases. RA is metabolized and deactivated by several enzymes, including cytochrome P450 (CYP) 26A1 and CYP26B1. RA serves as a ligand for the retinoic acid receptors (RARα, β and γ) which together with retinoid x receptors (RXRα, β and γ) form heterodimeric transcription factor complexes that recognize retinoic acid response elements (RAREs) on target gene promoters.

There is a wealth of information relating to the role of RA in later stages of prostate development and during adult prostate homeostasis. For example, retinoids are required for normal prostate branching morphogenesis during early postnatal development, where they restrict branching and promote ductal differentiation (Aboseif et al., 1997; Seo et al., 1997). Additionally, prostate tissue expresses RARs during most stages of development in humans (Richter et al., 2002), rats (Aboseif et al., 1997; Huang et al., 1997; Prins et al., 2002) and mice (Dolle et al., 1990; Mollard et al., 2000), and the prostate maintains responsiveness to RA after puberty. Retinoids are required for homeostasis of mature prostate: consumption of a retinoid-deficient diet caused keratinization of prostate epithelium in adult rats (Wolbach and Howe, 1925) and keratinized prostate epithelium and squamous metaplasia in adult mice (Lohnes et al., 1993). There is also evidence that RAR activity may be linked to prostate growth, since nuclear localization of RARα and RARγ increases during benign prostate disease and prostate cancer in humans (Gyftopoulos et al., 2000; Richter et al., 2002) and in a rat prostate cancer model (Richter et al., 1999).

However, virtually nothing is known about the requirement for RA in the initial stages of prostate development from the UGS. There are several reasons to think that retinoids may be implicated in the mechanism of prostatic bud initiation. First, retinoids actively participate in the process of bud initiation in many other organs, including chick wing (Tickle et al., 1985), zebrafish pectoral fin (Grandel et al., 2002) and mouse limb (Niederreither et al., 1999), incisor (Kronmiller et al., 1995), lung (Desai et al., 2006; Desai et al., 2004) and pancreas (Martin et al., 2005). Second, vitamin A deficiency during rat embryogenesis prevents development of mature prostate (Wilson and Warkany, 1948). Third, prostate development in vitamin A-deficient rats can be restored upon vitamin A supplementation between E10-15, a time during

fetal development that immediately precedes prostatic bud initiation (Wilson et al., 1953). Fourth, gene deletion studies in transgenic mice implicate members of the retinoid synthesis and signaling pathway in embryonic mouse prostate development (Abu-Abed et al., 2001; Huang et al., 2002).

Objectives of the present study were to determine if retinoid signaling (1) occurs in the fetal male mouse UGS and (2) is implicated in the mechanism of prostatic bud initiation. Accordingly, we characterized the expression of retinoid-dependent RARE-*lacZ* activity in the UGS of transgenic male mouse fetuses from E14.5 to E18.5. We also describe the distribution of retinoid synthesis gene expression (*Aldh1a* isoforms), retinoid metabolism gene expression (*Cyp26a1* and *b1*) and the expression of retinoid receptors (RARs and RXRs) in the fetal male mouse UGS during this same period of gestation. We show that RA added directly to fetal male mouse UGS organ culture media stimulates prostatic bud formation and alters the mRNA abundance of several genes implicated in the budding process, including the orphan nuclear receptor subfamily member f2 (*Nr2f2*), sonic hedgehog (*Shh*), and bone morphogenetic protein 4 (*Bmp4*). Taken together these results reveal that active retinoid signaling occurs in UGS mesenchyme during prostatic bud initiation, that RA is capable of increasing the number of prostatic buds, and that the mechanism for increased budding is associated with the coordinated increase in SHH and decrease in BMP4 signaling.

RESULTS

Localization of Retinoid Activity in Male Mouse UGS

We used a combination of whole-mount and tissue section imaging to investigate the distribution of retinoid signaling during embryonic prostate development from the UGS in Tg (RARE-Hspa1b/lacZ)12Jrt transgenic mice (Rossant et al., 1991). These mice express *lacZ* under the control of a RARE, obtained from the promoter of the *Rarb* gene, inserted upstream of the minimal promoter of heat shock protein 1a. At all fetal and postnatal ages examined, retinoid activity in whole-mount tissues was greater in the UGS proper than in the urethra or bladder (Fig. 1A-D). The punctate pattern of retinoid-dependent *LacZ* expression suggested that RA-responsive cells were unevenly distributed throughout the UGS rather than clustered in specific bands of tissue. At E14.5, prominent retinoid-dependent *LacZ* activity was observed in urogenital sinus mesenchyme (UGM) (Fig. 1a') and very low-level retinoid activity was also detected in epithelial cells of the bladder and, at an even lower frequency, in urogenital sinus epithelium (UGE). This very low activity persisted in UGE until birth. Retinoid activity was highly concentrated in the ventral mesenchymal pad (VMP) at E16.5 (Fig. 1b"), which is the major site of *Fgf10* synthesis in the ventral UGS (Thomson and Cunha, 1999). *LacZ* activity in UGM intensified during the initiation of prostatic buds, between E16.5-17.5 (Fig. 1b' and 1c') and subsequently decreased in a proximal-distal fashion between E17.5 and birth. It dissipated first from UGM that was closest to UGE and last from the VMP and mesenchyme surrounding the distal tips of elongating prostatic buds (Fig. 1d').

Retinoid activity was also observed during embryonic and early postnatal development of the seminal vesicles. At E14.5, retinoid-dependent *LacZ* activity was detected in Wolffian-derived epithelium (WE) located above the dorsal surface of the UGS. Retinoid activity was also detected in seminal vesicle mesenchyme and epithelium at E16.5 and increased between E17.5 and birth. Retinoid activity in seminal vesicle epithelium displayed a proximal to distal gradient that was most intense at distal seminal vesicle tips (Fig. 1c' and 1d').

Expression of RARs and RXRs in Male Mouse UGS

To determine which RAR isoforms were expressed in the UGS during prostatic bud initiation, we examined RARα, β and γ expression on E16.5, when prostatic buds first emerge from the

UGS. To determine which retinoid receptors were expressed in UGM, the UGS tissue component that most strongly exhibited retinoid activity in RARE-*LacZ* reporter mouse UGS, UGM, was isolated from E16.5 mouse UGSs ($n = 5$ separate fetuses), and pooled cDNA derived from these tissues was analyzed by RT-PCR. Analysis of *Krt14* mRNA, an epithelial marker not expressed in UGS mesenchyme, ensured that the purified UGM preparation was not contaminated with UGE (Fig. 2). Transcripts for all six *Rar* and *Rxr* isoforms were detected in E16.5 male mouse UGM (Fig. 2). To determine which RAR proteins were expressed in the UGS during prostatic bud initiation at E16.5, RAR and RXR expression were examined by immunoblotting of pooled protein from $n = 5$ whole UGSs. Protein bands corresponding to the correct sizes for RARα and γ and RXRα and γ were detected, but RAR β and RXR β were not detected in E16.5 UGS (Fig. 2). RARβ and RXRβ were detectable in E14.5 mouse limb protein preparations (Ghyselinck et al., 1997) that were run simultaneously with UGS proteins as a positive control (results not shown), so it is likely that these particular retinoid receptor proteins are truly absent from UGS. We observed strong IHC staining of UGS tissue sections stained for RAR and RXR proteins (not shown), however, we were unable to identify specific patterns of RAR and RXR proteins. Our experience is consistent with a previously reported lack of specificity in the available RAR and RXR antibodies that makes them unsuitable for IHC (Vernet et al., 2006).

Expression Patterns of RA Synthesis and Metabolism Enzymes in Male Mouse UGS

Aldehyde dehydrogenases (ALDHs) are responsible for the oxidation of retinaldehyde to its biologically active metabolite, RA. The expression and distribution of *Aldh1a1*, *a2* and *a3* was evaluated during UGS development by sectional and whole-mount ISH to determine whether the UGS maintains RA synthesis activity during prostatic bud initiation (Fig. 3). All three *Aldh* isoforms were expressed in the UGS at E15.5-17, each in a unique expression pattern that changed over the time course of prostatic bud initiation. At E15.5, before the initiation of prostatic buds, Wolffian-derived mesenchyme predominantly expressed *Aldh1a2*, while UGS and urethral mesenchyme predominantly expressed *Aldh1a2* and *a3*. Conversely, while UGS and urethral epithelium each expressed *Aldh1a1*, Wolffian-derived epithelium expressed *Aldh1a3* abundantly, as well as *Aldh1a1*. During prostatic bud initiation (E16.5) the abundance of all three *Aldh* isoforms decreased relative to their expression at E15.5. At E17.5, during prostatic bud elongation, *Aldh1a2* was strongly expressed in the periurethral prostatic mesenchyme at the distal tips of elongating prostatic buds and in inter-bud periurethral prostatic mesenchyme, while *Aldh1a1* and *a3* were more concentrated in inter-bud periurethral prostatic mesenchyme (Tissue sections in Fig. 3 and whole-mount ISH, not shown). These patterns of *Aldh* expression relative to the proximodistal prostatic bud axes was also observed at birth (P0.5). Also at this time, *Aldh1a1* became localized to the periurethral UGM, *Aldh1a2* was localized to UGM surrounding prostatic bud tips, and *Aldh1a3* was most abundant in urethral mesenchyme, but was also expressed in the periurethral UGM.

From these results, it appears that the ability to locally synthesize RA from retinol exists in the male mouse UGS and that retinoid signaling is both ongoing and region-specific during UGS development *in vivo*. In some developing organs, such as the testes (Vernet et al., 2006) and retina (McCaffery et al., 1999), the RA metabolizing enzymes cytochrome P450 (CYP) 26A1 and 26B1 act in conjunction with ALDH enzymes to establish gradients of retinoid activity. Expression of *Cyp26a1* and *b1* mRNAs was evaluated in E15.5-17 UGS tissue sections by ISH (Fig. 4). *Cyp26a1* was only weakly expressed in the UGS at the stages examined, but its expression pattern was region-specific and was also above the limit of detection, as determined by ISH with a *Cyp26a1* sense (control) probe (results not shown). Between E15.5-17.5, *Cyp26a1* expression was most abundant in mesenchyme on the ventral surface of the bladder neck, but was also detected at lower levels throughout the UGM and Wolffian-derived

mesenchyme. *Cyp26b1* was expressed in urethral and bladder mesenchyme in a discontinuous band of ventral UGM that was reciprocal to the pattern of *Aldh1a2* (Fig. 3) at this stage.

RA induced a classical transcriptional response in UGS organ culture

Exogenously administered RA is teratogenic and inhibits testicular steroidogenesis in developing rats (Livera et al., 2004; Livera et al., 2000). Since androgens are required for prostatic bud formation, it is difficult to assess direct effects of RA on prostatic bud formation *in utero* in the absence of confounding changes in circulating androgens. Therefore, we used an *in vitro* UGS organ culture model which allowed us to fix the concentration of androgen and vary the concentration of RA in culture medium. The UGS has the ability to synthesize, and metabolize RA and because retinoid signaling is active in UGS mesenchyme during the period of prostatic bud initiation, we first examined whether the UGS was capable of responding to exogenous RA in organ culture. UGSs were obtained from E14.5 male C57BL/6J mouse fetuses and incubated for 24 h in organ culture media containing 10 nM DHT and graded concentrations of RA (0-10 μM). Two known retinoid-related genes showed changes in expression. Abundance of *Cyp26b1* mRNA, an RA-metabolizing gene, was significantly increased at 1 μM RA while expression of *Nr2f2*, a potent transcriptional repressor that mediates biological effects of RA in many organ systems (Cooney et al., 1993) was decreased in a concentration-dependent manner (Fig. 5).

RA induced reciprocal changes in the mRNA abundance of Shh *and* Bmp4 *in the UGS and increased prostatic bud formation*

To determine whether RA was capable of inducing prostatic buds *in vitro*, UGSs were obtained from E14.5 male C57BL/6J mouse fetuses and incubated for 3 d in organ culture media containing 10 nM DHT and graded concentrations of RA (0-10 μM). Prostatic budding was evaluated after the 3 d culture period by removing the UGS mesenchyme, observing epithelial prostatic buds by scanning electron microscopy (SEM) and counting the total number of prostatic buds per UGS (Fig. 6).

RA stimulated prostatic budding in a concentration-dependent fashion (Fig. 7). Bud number was unchanged by low concentrations of RA (0-100 nM), but was significantly increased (1.7-fold) by 1 μM RA and further increased (2.2-fold) by 10 μM RA. Incubation of male UGSs (E14.5) in androgen-free organ culture containing RA (10 μM) for 3 d failed to induce prostatic budding (results not shown), demonstrating that androgens are required for stimulation of prostatic budding by RA.

To identify potential mechanisms for RA-induced prostatic budding, we examined the effect of RA on expression of genes implicated in the budding process. E14.5 UGSs were exposed in UGS organ culture to graded concentrations of RA (0-10 μM) for 24 h. Despite the well-recognized role of FGF10 in prostatic budding and the co-localization of abundant *Fgf10* expression and RARE-*LacZ* activity in the VMP, *Fgf10* mRNA expression was not RA-responsive (results not shown). In contrast, we found that RA exerted reciprocal effects on two other factors implicated as regulators of prostatic budding: sonic hedgehog (*Shh*) and bone morphogenetic protein 4 (*Bmp4*). RA increased *Shh* relative mRNA abundance at the highest concentration tested while decreasing *Bmp4* relative mRNA abundance at all concentrations (Fig. 7). Since the potency of RA for inducing prostatic buds was different from its potency for inducing *Shh* and repressing *Bmp4*, we assessed whether the ratio of *Shh/Bmp4* more closely correlated with the RA-inducible prostatic budding response. The *Shh/Bmp4* ratio was significantly increased at 1 μM RA; the lowest RA concentration that increased budding (Fig. 7). Hh signaling has been identified as a positive regulator of normal budding (Doles et al., 2006;Lamm et al., 2002;Podlasek et al., 1999) while BMP4 has been shown to be an inhibitor of prostatic budding (Almahbobi et al., 2005;Lamm et al., 2001). Thus, the RA induced increase

in prostatic bud formation may be mediated by reciprocal changes in expression of *Shh* and *Bmp4*.

To test this hypothesis, we examined the effect of exogenously induced changes in SHH or BMP4 signaling on prostatic bud induction (Fig. 8). UGSs were obtained from E14.5 male C57BL/6J mouse fetuses and incubated for 3 d in organ culture media containing 10 nM DHT and either NOGGIN (1 μg/ml; to block BMP signaling), SHH (5 μM) or SHH+NOGGIN. Prostatic budding was evaluated after the 3 d culture period by removing the UGS mesenchyme, observing epithelial prostatic buds by SEM and counting the total number of prostatic buds per UGS. Treatment with NOGGIN significantly increased prostatic budding. Treatment with exogenous SHH also significantly increased prostatic budding. Budding was also increased by co-treatment with the same concentrations of NOGGIN + SHH, respectively, but we did not observe an additive effect as compared to either factor alone.

DISCUSSION

This is the first study to demonstrate that RA can directly regulate the earliest stage of prostate morphogenesis—the initiation of prostatic buds. By using an *in vitro* culture system that circumvents the inhibitory effect of RA on testicular steroidogenesis, we were able to demonstrate that RA induces supernumerary prostatic budding from the fetal male mouse UGS in the presence of DHT. Moreover dynamic expression patterns of RAR and RXR proteins, *Aldh1a* genes, and *Cyp26* genes during normal prostatic bud initiation suggests that RA might be responsible for regulating prostatic budding *in situ*.

The developmental biology of retinoids has been studied for over 75 years and it is surprising that the involvement of RA in prostatic bud formation has not been described previously. However, there are several reasons that this effect of RA may have been overlooked. Wilson and co-workers (Wilson and Warkany, 1948; Wilson et al., 1953) described a syndrome resulting from maternal hypovitaminosis A in rats that included hypoplastic UGS, but the authors did not examine prostatic buds in these studies. Prostatic budding defects were not reported in mice deficient in any single RAR isoform (Maden, 2000) or in compound mutants (Luo et al., 1996), but functional redundancy among the RAR isoforms makes it impossible to exclude retinoid signaling from involvement in prostatic bud formation. Prostatic budding defects were not reported in targeted RXRα knockout mice (Huang et al., 2002), but the CRE-LOX system used to generate RXRα-null mice depended on expression of a prostate gene promoter that was only expressed postnatally (probasin) and was not appropriate for analysis of prostatic budding during fetal development. It is impossible to determine whether *Aldh1a2* knockout mice would exhibit prostatic budding defects since they die during mid-gestation (Mic et al., 2002), before prostate morphogenesis occurs. Other studies have examined the effects of *in utero* retinoid exposure on prostate morphogenesis (Robens, 1970). While exposure to excess RA during development caused hyperkeratinization of the prostate in rats and hamsters, formation of supernumerary prostate buds was not described as a characteristic feature of the hypervitaminosis A syndrome. More recently it was found that developmental exposure to excess RA arrests testicular steroidogenesis (Livera et al., 2004; Livera et al., 2000) in male mouse fetuses, and since androgens are required for prostatic bud initiation, *in utero* RA exposure is not an appropriate model for determining the role of RA in prostatic bud formation.

The effective concentration of RA that induced prostatic budding in organ culture in this study, particularly the 10 μM concentration, exceeded reported physiological levels in other developing mouse tissues where retinoids play a role in morphogenesis. Horton and Maden (1995) characterized RA concentrations in various tissues of the E13.5 mouse embryo by HPLC. RA concentrations ranged from 10-120 nM. Their reported concentration of RA in

mouse limb bud, 29 nM, was within range of that reported previously by Satre and Kochhar (1989), 0.3 ng/mg protein, and almost identical to that found in the chick limb bud by McCaffery et al. (1992), 25 nM. However, efforts to quantitate retinoid levels in specific organs are complicated by the fact that RA is not uniformly distributed, but rather localized to specific 'hotspots' of concentration (McCaffery et al., 1992; Thaller and Eichele, 1987). This appears to be true in the mouse UGS, where retinoid activity is localized to punctate islands within UGS mesenchyme. Even though concentrations of RA in this study are similar to those used in other organ culture studies (Galdones et al., 2006; Lambrot et al., 2006; Lasnitzki and Goodman, 1974; Lateef et al., 2004; Vilar et al., 1996) we do not know how they compare to endogenous retinoid concentrations in UGS tissues during *in utero* development. The kinetics of retinoid degradation is unknown in UGS organ culture and the concentration of RA in organ culture media is likely reduced by adherence to the polystyrene culture dish, which could decrease bioavailability by up to 40% (Kane et al., 2005).

Stimulation of prostatic budding by RA raises the question of what determines the number of prostatic buds that form during prostate development. Prostatic buds emerge in a temporally- and spatially-restricted manner that is determined largely by UGM identity: UGM from the dorsolateral UGS surface stimulates prostatic buds that mature into dorsolateral prostate ducts (Hayashi et al., 1993). Likewise, isolated mesenchyme from the ventral UGS surface stimulates formation of ventral prostate ducts (Timms et al., 1995). Therefore, the UGM is positionally patterned to specify prostatic budding regions that give rise to the various prostate lobes. This suggests the existence of non-bud-inducing UGM in the margins between buds. One possible explanation for induction of ectopic prostatic budding by RA in UGS organ culture is that RA affects UGS mesenchyme patterning and indirectly confers additional or expanded zones of competence for bud induction. In support of this possibility, there are numerous examples of RA re-specifying positional identity of inductive mesenchyme during development. Exposure of presomitic mesoderm to exogenous RA modified somite size in developing chicken and quail embryos (Diez del Corral et al., 2003; Maden, 2000). *In utero* exposure to RA reduced distal limb bud mesenchymal cell proliferation, reduced digit number and shortened long bones in the developing mouse autopod (Hayes and Morriss-Kay, 2001). Re-specification of limb bud mesenchymal identity was also observed during RA exposure of developing chick limbs (Tickle, 1991) and regenerating newt limbs (Pecorino et al., 1996). Local administration of RA in the presumptive hindbrain of developing chick embryos altered mesodermal homeobox gene expression and induced ectopic cartilage formation (Plant et al., 2000). Since transgenic loss of *Hoxd13* has been shown to decrease the number of dorsolateral buds (Podlasek et al., 1997), it seems quite plausible that RA induced changes in *Hox* gene expression and UGS patterning could result in additional or expanded domains of budding and supernumerary bud formation. Lin et al (2003) demonstrated the C67BL/6J male mouse UGS reproducibly displays 8 ventral buds, an average of 52 dorsolateral buds and 5-6 anterior buds on E18.5, but since the three dimensional UGS shape is distorted during incubation in UGS organ culture, the regional identity of buds cannot be reliably determined. Therefore, it was not possible to determine from the present study whether the induction of supernumerary prostatic buds by RA was restricted to specific lobes, interlobular boundary regions, or a generalized effect on the UGS as a whole.

Our finding that RA altered *Shh* and *Bmp4* expression in the UGS echoes previous observations that retinoid signaling perturbs their expression in other developing organs that undergo budding (Akimenko and Ekker, 1995; Helms et al., 1994; Wang et al., 2006). The mouse *Bmp4* promoter contains a RARE (Thompson et al., 2003) and the *Bmp4* expression domain in the UGS (Lamm et al., 2001) partially overlaps RAR-dependent retinoid activity described in this study. Therefore, BMP4 might be a primary RAR target gene in the UGS. In contrast, *Shh* expression is restricted to UGS epithelium (Podlasek et al., 1999) and does not overlap

RAR-dependent retinoid activity in the UGS. Accordingly, RA-induced changes in expression likely result from signaling between UGS mesenchyme and epithelium.

Supernumerary bud formation caused by RA in UGS organ culture was accompanied by reciprocal changes in *Shh* and *Bmp4* expression which, based on previous studies of their role in prostate budding, would be expected to favor bud formation. The role of SHH in prostate budding has been examined by several different investigators using chemical inhibitors, antibody blockade and transgenic *Shh*-null mice (Berman et al., 2004; Freestone et al., 2003; Lamm et al., 2002; Podlasek et al., 1999). Prostatic budding is normal in *Shh*-null mice (Freestone et al., 2003) and although cyclopamine decreases prostatic bud number in mouse UGS organ culture (Lamm et al., 2002) it does not completely block all prostatic buds from forming in rat UGS organ culture (Freestone et al., 2003). Interpretation of the above results is complicated by the potential for indian hedgehog and desert hedgehog, both of which are expressed in the developing mouse UGS, to provide functional redundancy for SHH signaling (see Doles et al., 2006 for a complete discussion). Thus, while SHH itself does not appear to be necessary for prostatic budding, uncertainty remains as to the requirement of Hh signaling in this process. The recent finding that prostatic budding is impaired in *Gli2* knockout mice provides the most compelling evidence that Hh signaling promotes prostatic bud formation (Doles et al., 2006; Lamm et al., 2002). None of the previous Hh research determined whether exogenous SHH was capable of inducing prostatic budding in the presence of DHT. The present study is the first to report that exogenous SHH stimulates prostatic bud formation in UGS organ culture when androgen is present in the medium.

In contrast to SHH, BMP4 has been identified as an inhibitor of prostate budding and branching. BMP4 inhibits budding in UGS organ culture and this effect can be overcome by the BMP antagonist NOGGIN (Cook et al., 2007; Lamm et al., 2001). Detailed analysis of the *Bmp4* null heterozygote showed that functional haploinsufficiency for *Bmp4* was associated with increased prostatic budding (Almahbobi et al., 2005) and increased indices of branching morphogenesis (Lamm et al., 2001). Our results show that, in the presence of DHT, SHH and the BMP4 antagonist NOGGIN induce supernumerary budding in the cultured UGS. Similarly, SHH induces supernumerary whisker buds in mice (Ohsaki et al., 2002) while either increased SHH signaling or blockade of BMP signaling during development of chick feather tracts (pterylae) both result in the formation of supplementary pterylae (Fliniaux et al., 2004). Further, the balance of BMP and SHH signaling has also been shown to be important for regulation of somite growth and development (Amthor et al., 1999), interneuron development from telencephalic progenitors (Gulacsi and Lillien, 2003) and establishment of dorsoventral boundaries in the developing eye (Sasagawa et al., 2002). Results both identifying SHH and BMP4 as potential regulators of budding and showing that perturbations of SHH and BMP4 signaling produce supernumerary buds support the hypothesis that RA-induced changes in their ratio may stimulate prostatic bud formation (Fig. 7).

However, while SHH, NOGGIN, and SHH + NOGGIN treatment of UGS organ cultures significantly increased prostatic bud number, we failed to observe an additive effect of SHH + NOGGIN. This was surprising as we expected co-treatment with these factors to produce the greatest ratio of SHH/BMP4 signaling. Nevertheless until we know (1) the full dose response curve for increasing budding by both SHH and NOGGIN alone, (2) the effect on bud formation of proportionately varied, graded concentrations of SHH and NOGGIN mixtures, and (3) the nature of the interaction between mixtures of SHH and NOGGIN (additive, synergistic, antagonistic, or no interaction) the notion that RA induced prostatic bud formation is regulated by the SHH/BMP4 ratio will remain a hypothesis.

The concentrations of SHH and NOGGIN used in UGS organ culture medium in the present study were considerable (Fig. 8). At these concentrations each one of these factors alone may

have elicited the maximal increase in prostatic bud formation by increasing the SHH/BMP4 signaling ratio. Since 10 μM RA was able to induce a greater number of prostatic buds than either SHH, NOGGIN, or cotreatment with SHH + NOGGIN (compare Figs. 7 and 8) it may be that RA exerts additional actions to over-ride this limit. In this regard the transcriptional repressor, NR2F2, is of interest. It acts on multiple signaling pathways by inhibiting SF1, USF and AP1 (Xing et al., 2002). NR2F2 is critical for limb bud outgrowth in mice (Lee et al., 2004), development of the inner ear, liver and pancreas (Tang et al., 2005;Zhang et al., 2002), as well as venous identity (You et al., 2005). *Nr2f2* is highly expressed in UGS mesenchyme during prostate development (Tsai and Tsai, 1997), but its role has not been defined. Whereas induction of *Nr2f2* expression by RA has been associated with RA-mediated teratogenesis and cell death (Chen et al., 2007;Lin et al., 2000) we observed repression of *Nr2f2* expression by RA. We speculate that NR2F2 might function as a potential "prostatic bud gatekeeper" in the UGS and that its repression by RA may act in concert with the enhanced SHH/BMP4 ratio to further increase budding.

In summary, results of the present study reveal dynamic patterns of RA signaling during early prostate development, show that RA induces supernumerary prostatic buds in UGS organ culture and correlate this effect with reciprocal changes in the expression of *Shh* and *Bmp4*. Thus, these findings support the notion that retinoids and associated retinoid-dependent genes may be important determinants for prostatic bud patterning and morphogenesis during early prostate development, but require additional studies addressing the role of physiologically-relevant retinoid levels during prostatic budding *in utero*. Additionally, the relationship between retinoid, BMP, and SHH signaling in RA induced prostatic bud formation has been raised but not resolved. Future studies will be needed to determine whether RA directly regulates *Shh* and *Bmp4* gene expression, to characterize the time course for their induction and repression, and to address whether proportionately varied, graded concentrations of SHH and NOGGIN mixtures in UGS organ culture medium are capable of producing an additive increase in prostatic bud formation.

EXPERIMENTAL PROCEDURES

Animals

C57BL/6J mice (Jackson Laboratory, Bar Harbor, ME) and Tg(RARE-Hspa1b/lacZ)12Jrt (Rossant et al., 1991) (bred onto the CD-1 strain and provided by Dr. Margaret Clagett-Dame, University of Wisconsin, Department of Biochemistry and School of Pharmacy) were housed in clear plastic cages containing corn cob bedding and maintained at 24±1 °C on a 12 h light and dark cycle. Feed (5013 LabDiet®, PMI Nutrition International, Brentwood, MO) and tap water were available *ad libitum*. All procedures were approved by the University of Wisconsin Animal Care and Use Committee and conducted in accordance with the NIH Guide for the Care and Use of Laboratory Animals. To obtain timed-pregnant dams, female mice were paired overnight with males. The next day was considered E0.5. Dams were euthanized by CO_2 asphyxiation and fetuses were maintained in phosphate buffered saline (PBS) prior to dissection. All results were based on data from at least three separate mouse litters per endpoint.

Assay for β-galactosidase activity

β-Galactosidase activity was determined as described previously (Cheng et al., 1993). At least $n = 3$ separate UGS or prostate specimens, each belonging to a male fetus or newborn from a separate litter, were assessed at each developmental stage. The tissue specimens were fixed for 20 min in ice-cold 1% glutaraldehyde, rinsed with PBS, and suspended in PBS containing 5 mM $K_3Fe(CN)_3$, 5 mM $K_4Fe(CN)_6$, 2 mM $MgCl_2$, 0.02% NP-40, 0.01% sodium deoxycholate, and 1 mg/ml X-gal. All tissues were incubated for exactly 30 min at 37 °C in the dark on a

rocking platform, washed with PBS, and imaged directly or cut into 80 μm sections using a vibratome before imaging by light microscopy.

UGS Organ Culture and Bud Counting

UGSs were dissected from E14.5 male C57BL/6J mouse fetuses in ice-cold PBS and placed on 0.4 μm Millicell-CM filters (Millipore, Billerica, MA) in tissue culture plates containing serum-free DMEM/F12 media supplemented with 2% insulin-transferrin-selenium solution, 25 μg/ml gentamicin, 0.25 μg/ml amphotericin B, 10 nM 5α-dihydrotestosterone (DHT), RA, recombinant SHH (5 μM; Curis, Cambridge, MA) or recombinant NOGGIN (1 μg/ml, R&D systems, Minneapolis, MN). Medium was changed every 2 d. Some UGS tissues were harvested after 1 d for RT-PCR analysis and frozen in liquid nitrogen. Other UGS specimens were harvested after 3 d in culture, enzymatically digested with 1% trypsin, and separated mechanically into UGS mesenchymal and UGS epithelial components. UGS epithelium was then fixed in 2.5% glutaraldehyde and evaluated by scanning electron microscopy (SEM). SEM was performed as previously described (Lin et al., 2003). UGS specimens were imaged from 4 angles to visualize budding across the entire UGS surface. Prostatic buds were counted by two blinded individuals and prostatic bud numbers were determined by averaging the total bud counts per UGS from these individuals. The significance of differences in mean prostatic bud number among exposure groups were determined by analysis of variance (ANOVA), followed by Fischer's least significant difference test ($p < 0.05$).

Immunoblotting

UGS tissues were homogenized in ice-cold lysis buffer (150 mM NaCl, 10 mM Tris, 1 mM EDTA, 1 mM EGTA, 1 mM Hepes, 1% Triton X-100, pH 7.5) containing protease inhibitors (2 μg/ml leupeptin, 2 μg/ml aprotinin, 2 mM sodium vanadate and 0.2 mM 4-aminidophenylmethane sulfonyl fluoride). Protein abundance was determined using the BCA method, according to manufacturer's instructions (Pierce, Rockford, IL). Ten milligrams of total protein were separated by SDS-PAGE and transferred to nitrocellulose membranes. Membranes were blocked in Tris-buffered saline containing 0.1% Tween-20 (TBST) and 5% nonfat dry milk for 1 h. RARs and RXRs were detected using the following antibodies from Santa Cruz Biotechnology, diluted 1:200 in TBST containing 3% nonfat dry milk and incubated overnight with the membrane: sc-551 rabbit polyclonal anti-RARα, sc-552 rabbit polyclonal anti-RARβ, sc-7387 mouse monoclonal anti-RARγ, sc-46659 mouse monoclonal anti-RXRα 1, sc-831 rabbit polyclonal anti-RXRβ 1 and sc-555 rabbit polyclonal anti-RXRγ 1. Membranes were washed with TBST and incubated with secondary antibodies (horseradish peroxidase-conjugated goat anti-mouse or goat anti-rabbit IgG (Vector Labs, Burlingame, CA), diluted 1:2000 in TBST containing 5% non-fat dry milk for 1 h. Membranes were washed in TBST and peroxidase activity was detected using the SuperSignal West Pico Chemiluminescent Substrate (Pierce) and CL-XPosure film (Pierce).

RNA Isolation and RT-PCR

UGS specimens were homogenized with the aid of Molecular Grinding Resin™ (Genotech, St. Louis, MO) and tissue homogenates were passed through Qiashredder columns (Qiagen, Valencia, CA). RNA was extracted from tissue homogenates with the Qiagen RNeasy kit (Qiagen). Reverse transcription was carried out for 1 h at 42°C in 1X first stand buffer containing 500 ng total RNA, 0.5 μM dNTPs, 150 ng random hexamers, 5 mM DTT and 200 U Superscript II reverse transcriptase (Invitrogen). PCR and real-time PCR reactions were assembled as described previously (Lin et al., 2003) and thermocylcing was performed using the GeneAmp 9600 (Perkin Elmer, Norkwalk, CT) or Roche LightCycler (Roche Molecular Biochemicals, Indianapolis, IN). PCR primers were as follows: *Cyp26b1*: 5′ -ATGACTGGGTGGAAGACGAG-3′ and 5′ -TGTTCTGTGTGGCTGGTGAG-3′, *Bmp4*: 5′ -

AACTGCCGTCGCCATTCACTATAC-3′ and 5′ -TGCACAATGGCATGGTTGGTTGAG-3′, *Nr2f2*: 5′ -GGGCTGGTGACAGAGGTGA-3′ and 5′ -GGGAAGCTGAGGGTCAGATAAAG-3′, and *Ppia*: 5′ -TCTCTCCGTAGATGGACCTG-3′ and 5′ -ATCACGGCCGATGACGAGCC-3′, *Rara*: 5′ -CGACCAGATCACCCTCCTC-3′ and 5′ -CAGTCCAGTCTCAGCATCGTC-3′,*Rarb*: 5′ -GTAGCCCAGTGTCCTTGCTG-3′ and 5′ - CTTGAGTCTGTCAACCACTCATTC-3′, *Rarg*: 5′ -GCAGGGCCCTCCTACACTAC-3′ and 5′ -GCCTGCAGGAATCTTATTTGG-3′,*Rxra*: 5′ - TCCTGTGGTCAGCTCCAGTC-3′ and 5′ -AGAAGCTGGGTGCAGGAAAG-3′,*Rxrb*: 5′ - CATTTGGCCTCACTCCCTTC-3′ and 5′ -AGAGCAATGGGTTCCTCCAC, *Rxrg*: 5′ -GCCCTACCCTGCACACTCTC-3′ and 5′ -TGGCCACTCTTCCCAAGAAC-3′, *Shh*: 5′ -GTGGAAGCAGGTTTCGACTG-3′ and 5′ -GGTCCAGGAAGGTGAGGAAG-3′.

Whole Mount and Sectional *In Situ* Hybridization (ISH)

UGS and prostate tissue were fixed overnight in 4% paraformaldehyde at 4°C. For ISH on tissue sections, UGS were embedded in 4% Sea Plaque agarose (Biowhittaker Molecular Applications, Rockland, ME) and sectioned (80 μm) in ice-cold phosphate-buffered saline containing 0.1% Tween 20, using a vibratome fitted with a double-edged razor blade. Whole-mount and sectional ISH were performed essentially as described previously (Lamm et al., 2001). Tissues were bleached with 6% H_2O_2 and digested with proteinase K. Prehybridization (2 h) and hybridization (overnight) were each performed at 60.5°C. After high-stringency washes, and blocking non-specific binding sites for 2 h, tissues were incubated overnight at 4° C in Tris-buffered saline containing 5% normal sheep serum, 1% blocking reagent (Roche), 1% BSA, and preblocked alkaline phosphatase-conjugated anti-digoxygenin (1:1000). The colorimetric reaction used BM purple solution (Indianapolis, IN) as a chromagen for sectional ISH and BCIP/NBT as a chromogen for whole-mount ISH. Whole-mount tissue imaging was performed in PBS containing 50% formamide. For each probe, the time allowed for color development was the same for all samples so that relative color intensity could be used as a marker for relative mRNA abundance. Probes for *Aldh 1a1*, *1a2*, and *1a3* were provided by Dr. Cathy Mendelsohn (Columbia University, New York, NY) and probes for *Cyp26a1* and *Cyp26b1* were provided by Dr. Margaret Clagett-Dame (University of Wisconsin, Madison, WI).

ACKNOWLEDGEMENTS

We thank Dr. Margaret Clagett-Dame (Univ. of Wisconsin, Dept. of Biochemistry and School of Pharmacy) for providing a breeding pair of *RARE-lacZ* mice and for assistance with research described in this manuscript, and Drs. Hui Li(University of Wisconsin) and Kwan-Hee Kim (Washington State Univ., School of Molecular Biosciences) for assistance with RAR antibodies.

Grant Information

This work was supported by the following grants from NIH: F32ES014284, F31HD049323, R37 ES01332, and DK065303.

REFERENCES

Aboseif SR, Dahiya R, Narayan P, Cunha GR. Effect of retinoic acid on prostatic development. Prostate 1997;31:161–7. [PubMed: 9167767]

Abu-Abed S, Dolle P, Metzger D, Beckett B, Chambon P, Petkovich M. The retinoic acid-metabolizing enzyme, CYP26A1, is essential for normal hindbrain patterning, vertebral identity, and development of posterior structures. Genes Dev 2001;15:226–40. [PubMed: 11157778]

Akimenko MA, Ekker M. Anterior duplication of the sonic hedgehog expression pattern in the pectoral fin buds of zebrafish treated with retinoic acid. Dev Biol 1995;170:243–7. [PubMed: 7601313]

Almahbobi G, Hedwards S, Fricout G, Jeulin D, Bertram JF, Risbridger GP. Computer-based detection of neonatal changes to branching morphogenesis reveals different mechanisms of and predicts prostate enlargement in mice haplo-insufficient for bone morphogenetic protein 4. J Pathol 2005;206:52–61. [PubMed: 15772937]

Amthor H, Christ B, Patel K. A molecular mechanism enabling continuous embryonic muscle growth - a balance between proliferation and differentiation. Development 1999;126:1041–53. [PubMed: 9927604]

Berman DM, Desai N, Wang X, Karhadkar SS, Reynon M, Abate-Shen C, Beachy PA, Shen MM. Roles for Hedgehog signaling in androgen production and prostate ductal morphogenesis. Dev Biol 2004;267:387–98. [PubMed: 15013801]

Chen J, Carney SA, Peterson RE, Heideman W. Retinoic acid induced cardiotoxicity in the zebrafish embryo: microarray studies identify *Nr2f5* as a critical target. Physiol Genomics. 2007In Press

Cheng TC, Wallace MC, Merlie JP, Olson EN. Separable regulatory elements governing myogenin transcription in mouse embryogenesis. Science 1993;261:215–8. [PubMed: 8392225]

Clagett-Dame M, DeLuca HF. The role of vitamin A in mammalian reproduction and embryonic development. Annu Rev Nutr 2002;22:347–81. [PubMed: 12055350]

Cook C, Vezina CM, Allgeier SH, Shaw A, Yu M, Peterson RE, Bushman W. Noggin is required for normal lobe patterning and ductal budding in the mouse prostate. Dev Biol 2007;312:217–30. [PubMed: 18028901]

Cooney AJ, Leng X, Tsai SY, O'Malley BW, Tsai MJ. Multiple mechanisms of chicken ovalbumin upstream promoter transcription factor-dependent repression of transactivation by the vitamin D, thyroid hormone, and retinoic acid receptors. J Biol Chem 1993;268:4152–60. [PubMed: 8382695]

Cunha GR, Donjacour AA, Cooke PS, Mee S, Bigsby RM, Higgins SJ, Sugimura Y. The endocrinology and developmental biology of the prostate. Endocr Rev 1987;8:338–62. [PubMed: 3308446]

Cunha GR, Lung B. The possible influence of temporal factors in androgenic responsiveness of urogenital tissue recombinants from wild-type and androgen-insensitive (*Tfm*) mice. J Exp Zool 1978;205:181–93. [PubMed: 681909]

Desai TJ, Chen F, Lu J, Qian J, Niederreither K, Dolle P, Chambon P, Cardoso WV. Distinct roles for retinoic acid receptors alpha and beta in early lung morphogenesis. Dev Biol 2006;291:12–24. [PubMed: 16427040]

Desai TJ, Malpel S, Flentke GR, Smith SM, Cardoso WV. Retinoic acid selectively regulates Fgf10 expression and maintains cell identity in the prospective lung field of the developing foregut. Dev Biol 2004;273:402–15. [PubMed: 15328022]

Diez del Corral R, Olivera-Martinez I, Goriely A, Gale E, Maden M, Storey K. Opposing FGF and retinoid pathways control ventral neural pattern, neuronal differentiation, and segmentation during body axis extension. Neuron 2003;40:65–79. [PubMed: 14527434]

Doles J, Cook C, Shi X, Valosky J, Lipinski R, Bushman W. Functional compensation in hedgehog signaling during mouse prostate development. Dev Biol 2006;295:13–25. [PubMed: 16707121]

Dolle P, Ruberte E, Leroy P, Morriss-Kay G, Chambon P. Retinoic acid receptors and cellular retinoid binding proteins. I. A systematic study of their differential pattern of transcription during mouse organogenesis. Development 1990;110:1133–51. [PubMed: 1966045]

Fliniaux I, Viallet JP, Dhouailly D. Signaling dynamics of feather tract formation from the chick somatopleure. Development 2004;131:3955–66. [PubMed: 15269169]

Freestone SH, Marker P, Grace OC, Tomlinson DC, Cunha GR, Harnden P, Thomson AA. Sonic hedgehog regulates prostatic growth and epithelial differentiation. Dev Biol 2003;264:352–62. [PubMed: 14651923]

Galdones E, Lohnes D, Hales BF. Role of retinoic acid receptors alpha1 and gamma in the response of murine limbs to retinol in vitro. Birth Defects Res A Clin Mol Teratol 2006;76:39–45. [PubMed: 16397886]

Ghyselinck NB, Dupe V, Dierich A, Messaddeq N, Garnier JM, Rochette-Egly C, Chambon P, Mark M. Role of the retinoic acid receptor beta (RARbeta) during mouse development. Int J Dev Biol 1997;41:425–47. [PubMed: 9240560]

Goldstein JL, Wilson JD. Genetic and hormonal control of male sexual differentiation. J Cell Physiol 1975;85:365–77. [PubMed: 164477]

Grandel H, Lun K, Rauch GJ, Rhinn M, Piotrowski T, Houart C, Sordino P, Kuchler AM, Schulte-Merker S, Geisler R, Holder N, Wilson SW, Brand M. Retinoic acid signalling in the zebrafish embryo is necessary during pre-segmentation stages to pattern the anterior-posterior axis of the CNS and to induce a pectoral fin bud. Development 2002;129:2851–65. [PubMed: 12050134]

Grishina IB, Kim SY, Ferrara C, Makarenkova HP, Walden PD. BMP7 inhibits branching morphogenesis in the prostate gland and interferes with Notch signaling. Dev Biol 2005;288:334–47. [PubMed: 16324690]

Gulacsi A, Lillien L. Sonic hedgehog and bone morphogenetic protein regulate interneuron development from dorsal telencephalic progenitors *in vitro*. J Neurosci 2003;23:9862–72. [PubMed: 14586015]

Gyftopoulos K, Perimenis P, Sotiropoulou-Bonikou G, Sakellaropoulos G, Varakis I, Barbalias GA. Immunohistochemical detection of retinoic acid receptor-alpha in prostate carcinoma: correlation with proliferative activity and tumor grade. Int Urol Nephrol 2000;32:263–9. [PubMed: 11229646]

Hayashi N, Cunha GR, Parker M. Permissive and instructive induction of adult rodent prostatic epithelium by heterotypic urogenital sinus mesenchyme. Epithelial Cell Biol 1993;2:66–78. [PubMed: 8353595]

Hayes C, Morriss-Kay GM. Retinoic acid specifically downregulates *Fgf4* and inhibits posterior cell proliferation in the developing mouse autopod. J Anat 2001;198:561–8. [PubMed: 11430695]

Helms J, Thaller C, Eichele G. Relationship between retinoic acid and sonic hedgehog, two polarizing signals in the chick wing bud. Development 1994;120:3267–74. [PubMed: 7720566]

Horton C, Maden M. Endogenous distribution of retinoids during normal development and teratogenesis in the mouse embryo. Dev Dyn 1995;202:312–23. [PubMed: 7780180]

Huang HF, Li MT, Von Hagen S, Zhang YF, Irwin RJ. Androgen modulation of the messenger ribonucleic acid of retinoic acid receptors in the prostate, seminal vesicles, and kidney in the rat. Endocrinology 1997;138:553–9. [PubMed: 9002985]

Huang J, Powell WC, Khodavirdi AC, Wu J, Makita T, Cardiff RD, Cohen MB, Sucov HM, Roy-Burman P. Prostatic intraepithelial neoplasia in mice with conditional disruption of the retinoid X receptor alpha allele in the prostate epithelium. Cancer Res 2002;62:4812–9. [PubMed: 12183441]

Kane MA, Chen N, Sparks S, Napoli JL. Quantification of endogenous retinoic acid in limited biological samples by LC/MS/MS. Biochem J 2005;388:363–9. [PubMed: 15628969]

Kronmiller JE, Nguyen T, Berndt W. Instruction by retinoic acid of incisor morphology in the mouse embryonic mandible. Arch Oral Biol 1995;40:589–95. [PubMed: 7575229]

Lambrot R, Coffigny H, Pairault C, Donnadieu AC, Frydman R, Habert R, Rouiller-Fabre V. Use of organ culture to study the human fetal testis development: effect of retinoic acid. J Clin Endocrinol Metab 2006;91:2696–703. [PubMed: 16621909]

Lamm ML, Catbagan WS, Laciak RJ, Barnett DH, Hebner CM, Gaffield W, Walterhouse D, Iannaccone P, Bushman W. Sonic hedgehog activates mesenchymal Gli1 expression during prostate ductal bud formation. Dev Biol 2002;249:349–66. [PubMed: 12221011]

Lamm ML, Podlasek CA, Barnett DH, Lee J, Clemens JQ, Hebner CM, Bushman W. Mesenchymal factor bone morphogenetic protein 4 restricts ductal budding and branching morphogenesis in the developing prostate. Dev Biol 2001;232:301–14. [PubMed: 11401393]

Lasnitzki I, Goodman DS. Inhibition of the effects of methylcholanthrene on mouse prostate in organ culture by vitamin A and its analogs. Cancer Res 1974;34:1564–71. [PubMed: 4833910]

Lasnitzki I, Mizuno T. Prostatic induction: interaction of epithelium and mesenchyme from normal wild-type mice and androgen-insensitive mice with testicular feminization. J Endocrinol 1980;85:423–8. [PubMed: 7411008]

Lateef H, Stevens MJ, Varani J. All-trans-retinoic acid suppresses matrix metalloproteinase activity and increases collagen synthesis in diabetic human skin in organ culture. Am J Pathol 2004;165:167–74. [PubMed: 15215172]

Lee CT, Li L, Takamoto N, Martin JF, Demayo FJ, Tsai MJ, Tsai SY. The nuclear orphan receptor COUP-TFII is required for limb and skeletal muscle development. Mol Cell Biol 2004;24:10835–43. [PubMed: 15572686]

Lin B, Chen GQ, Xiao D, Kolluri SK, Cao X, Su H, Zhang XK. Orphan receptor COUP-TF is required for induction of retinoic acid receptor beta, growth inhibition, and apoptosis by retinoic acid in cancer cells. Mol Cell Biol 2000;20:957–70. [PubMed: 10629053]

Lin TM, Rasmussen NT, Moore RW, Albrecht RM, Peterson RE. Region-specific inhibition of prostatic epithelial bud formation in the urogenital sinus of C57BL/6 mice exposed *in utero* to 2,3,7,8-tetrachlorodibenzo-*p*-dioxin. Toxicol Sci 2003;76:171–81. [PubMed: 12944588]

Livera G, Pairault C, Lambrot R, Lelievre-Pegorier M, Saez JM, Habert R, Rouiller-Fabre V. Retinoid-sensitive steps in steroidogenesis in fetal and neonatal rat testes: *in vitro* and *in vivo* studies. Biol Reprod 2004;70:1814–21. [PubMed: 14960491]

Livera G, Rouiller-Fabre V, Durand P, Habert R. Multiple effects of retinoids on the development of sertoli, germ, and leydig cells of fetal and neonatal rat testis in culture. Biol Reprod 2000;62:1303–14. [PubMed: 10775181]

Lohnes D, Kastner P, Dierich A, Mark M, LeMeur M, Chambon P. Function of retinoic acid receptor gamma in the mouse. Cell 1993;73:643–58. [PubMed: 8388780]

Luo J, Sucov HM, Bader JA, Evans RM, Giguere V. Compound mutants for retinoic acid receptor (RAR) beta and RAR alpha 1 reveal developmental functions for multiple RAR beta isoforms. Mech Dev 1996;55:33–44. [PubMed: 8734497]

Maden M. The role of retinoic acid in embryonic and post-embryonic development. Proc Nutr Soc 2000;59:65–73. [PubMed: 10828175]

Martin M, Gallego-Llamas J, Ribes V, Kedinger M, Niederreither K, Chambon P, Dolle P, Gradwohl G. Dorsal pancreas agenesis in retinoic acid-deficient *Raldh2* mutant mice. Dev Biol 2005;284:399–411. [PubMed: 16026781]

McCaffery P, Lee MO, Wagner MA, Sladek NE, Drager UC. Asymmetrical retinoic acid synthesis in the dorsoventral axis of the retina. Development 1992;115:371–82. [PubMed: 1425331]

McCaffery P, Wagner E, O'Neil J, Petkovich M, Drager UC. Dorsal and ventral retinal territories defined by retinoic acid synthesis, break-down and nuclear receptor expression. Mech Dev 1999;82:119–30. [PubMed: 10354476]

Mic FA, Haselbeck RJ, Cuenca AE, Duester G. Novel retinoic acid generating activities in the neural tube and heart identified by conditional rescue of *Raldh2* null mutant mice. Development 2002;129:2271–82. [PubMed: 11959834]

Mollard R, Viville S, Ward SJ, Decimo D, Chambon P, Dolle P. Tissue-specific expression of retinoic acid receptor isoform transcripts in the mouse embryo. Mech Dev 2000;94:223–32. [PubMed: 10842077]

Niederreither K, Subbarayan V, Dolle P, Chambon P. Embryonic retinoic acid synthesis is essential for early mouse post-implantation development. Nat Genet 1999;21:444–8. [PubMed: 10192400]

Ohsaki K, Osumi N, Nakamura S. Altered whisker patterns induced by ectopic expression of *Shh* are topographically represented by barrels. Brain Res Dev Brain Res 2002;137:159–70.

Pecorino LT, Brockes JP, Entwistle A. Semi-automated positional analysis using laser scanning microscopy of cells transfected in a regenerating newt limb. J Histochem Cytochem 1996;44:559–69. [PubMed: 8666741]

Plant MR, MacDonald ME, Grad LI, Ritchie SJ, Richman JM. Locally released retinoic acid repatterns the first branchial arch cartilages in vivo. Dev Biol 2000;222:12–26. [PubMed: 10885743]

Podlasek CA, Barnett DH, Clemens JQ, Bak PM, Bushman W. Prostate development requires Sonic hedgehog expressed by the urogenital sinus epithelium. Dev Biol 1999;209:28–39. [PubMed: 10208740]

Podlasek CA, Duboule D, Bushman W. Male accessory sex organ morphogenesis is altered by loss of function of Hoxd-13. Dev Dyn 1997;208:454–65. [PubMed: 9097018]

Prins GS, Chang WY, Wang Y, van Breemen RB. Retinoic acid receptors and retinoids are up-regulated in the developing and adult rat prostate by neonatal estrogen exposure. Endocrinology 2002;143:3628–40. [PubMed: 12193579]

Richter F, Huang HF, Li MT, Danielpour D, Wang SL, Irwin RJ Jr. Retinoid and androgen regulation of cell growth, epidermal growth factor and retinoic acid receptors in normal and carcinoma rat prostate cells. Mol Cell Endocrinol 1999;153:29–38. [PubMed: 10459851]

Richter F, Joyce A, Fromowitz F, Wang S, Watson J, Watson R, Irwin RJ Jr. Huang HF. Immunohistochemical localization of the retinoic acid receptors in human prostate. J Androl 2002;23:830–8. [PubMed: 12399530]

Robens JF. Teratogenic effects of hypervitaminosis A in the hamster and the guinea pig. Toxicol Appl Pharmacol 1970;16:88–99. [PubMed: 5416756]

Rossant J, Zirngibl R, Cado D, Shago M, Giguere V. Expression of a retinoic acid response element-*hsplacZ* transgene defines specific domains of transcriptional activity during mouse embryogenesis. Genes Dev 1991;5:1333–44. [PubMed: 1907940]

Saito M, Mizuno T. Prostatic bud induction by brief treatment with growth factors. C R Seances Soc Biol Fil 1997;191:261–5. [PubMed: 9255353]

Sasagawa S, Takabatake T, Takabatake Y, Muramatsu T, Takeshima K. Axes establishment during eye morphogenesis in Xenopus by coordinate and antagonistic actions of BMP4, Shh, and RA. Genesis 2002;33:86–96. [PubMed: 12112877]

Satre MA, Kochhar DM. Elevations in the endogenous levels of the putative morphogen retinoic acid in embryonic mouse limb-buds associated with limb dysmorphogenesis. Dev Biol 1989;133:529–36. [PubMed: 2731639]

Seo R, McGuire M, Chung M, Bushman W. Inhibition of prostate ductal morphogenesis by retinoic acid. J Urol 1997;158:931–5. [PubMed: 9258121]

Tang LS, Alger HM, Lin F, Pereira FA. Dynamic expression of COUP-TFI and COUP-TFII during development and functional maturation of the mouse inner ear. Gene Expr Patterns 2005;5:587–92. [PubMed: 15907456]

Thaller C, Eichele G. Identification and spatial distribution of retinoids in the developing chick limb bud. Nature 1987;327:625–8. [PubMed: 3600758]

Thompson DL, Gerlach-Bank LM, Barald KF, Koenig RJ. Retinoic acid repression of bone morphogenetic protein 4 in inner ear development. Mol Cell Biol 2003;23:2277–86. [PubMed: 12640113]

Thomson AA, Cunha GR. Prostatic growth and development are regulated by FGF10. Development 1999;126:3693–701. [PubMed: 10409514]

Tickle C. Retinoic acid and chick limb bud development. Dev Suppl 1991;1:113–21. [PubMed: 1683800]

Tickle C, Lee J, Eichele G. A quantitative analysis of the effect of all-trans-retinoic acid on the pattern of chick wing development. Dev Biol 1985;109:82–95. [PubMed: 3987968]

Timms BG, Lee CW, Aumuller G, Seitz J. Instructive induction of prostate growth and differentiation by a defined urogenital sinus mesenchyme. Microsc Res Tech 1995;30:319–32. [PubMed: 7606051]

Tsai SY, Tsai MJ. Chick ovalbumin upstream promoter-transcription factors (COUP-TFs): coming of age. Endocr Rev 1997;18:229–40. [PubMed: 9101138]

Vernet N, Dennefeld C, Rochette-Egly C, Oulad-Abdelghani M, Chambon P, Ghyselinck NB, Mark M. Retinoic acid metabolism and signaling pathways in the adult and developing mouse testis. Endocrinology 2006;147:96–110. [PubMed: 16210368]

Vilar J, Gilbert T, Moreau E, Merlet-Benichou C. Metanephros organogenesis is highly stimulated by vitamin A derivatives in organ culture. Kidney Int 1996;49:1478–87. [PubMed: 8731117]

vom Saal FS, Timms BG, Montano MM, Palanza P, Thayer KA, Nagel SC, Dhar MD, Ganjam VK, Parmigiani S, Welshons WV. Prostate enlargement in mice due to fetal exposure to low doses of estradiol or diethylstilbestrol and opposite effects at high doses. Proc Natl Acad Sci U S A 1997;94:2056–61. [PubMed: 9050904]

Wang Z, Dolle P, Cardoso WV, Niederreither K. Retinoic acid regulates morphogenesis and patterning of posterior foregut derivatives. Dev Biol 2006;297:433–45. [PubMed: 16806149]

Warot X, Fromental-Ramain C, Fraulob V, Chambon P, Dolle P. Gene dosage-dependent effects of the Hoxa-13 and Hoxd-13 mutations on morphogenesis of the terminal parts of the digestive and urogenital tracts. Development 1997;124:4781–91. [PubMed: 9428414]

Wilson JD, Warkany J. Malformations in the genitor-urinary tract induced by maternal vitamin A deficiency in the rat. Am J Anat 1948;88:357–407. [PubMed: 18098411]

Wilson JG, Roth CB, Warkany J. An analysis of the syndrome of malformations induced by maternal vitamin A deficiency. Effects of restoration of vitamin A at various times during gestation. Am J Anat 1953;92:189–217. [PubMed: 13030424]

Wolbach SB, Howe PR. Tissue changes following deprivation of fat-soluble A vitamin. J Exp Med 1925;42:753–777.

Xing W, Danilovich N, Sairam MR. Orphan receptor chicken ovalbumin upstream promoter transcription factors inhibit steroid factor-1, upstream stimulatory factor, and activator protein-1 activation of ovine follicle-stimulating hormone receptor expression via composite cis-elements. Biol Reprod 2002;66:1656–66. [PubMed: 12021044]

You LR, Lin FJ, Lee CT, DeMayo FJ, Tsai MJ, Tsai SY. Suppression of Notch signalling by the COUP-TFII transcription factor regulates vein identity. Nature 2005;435:98–104. [PubMed: 15875024]

Zhang P, Bennoun M, Gogard C, Bossard P, Leclerc I, Kahn A, Vasseur-Cognet M. Expression of COUP-TFII in metabolic tissues during development. Mech Dev 2002;119:109–14. [PubMed: 12385758]

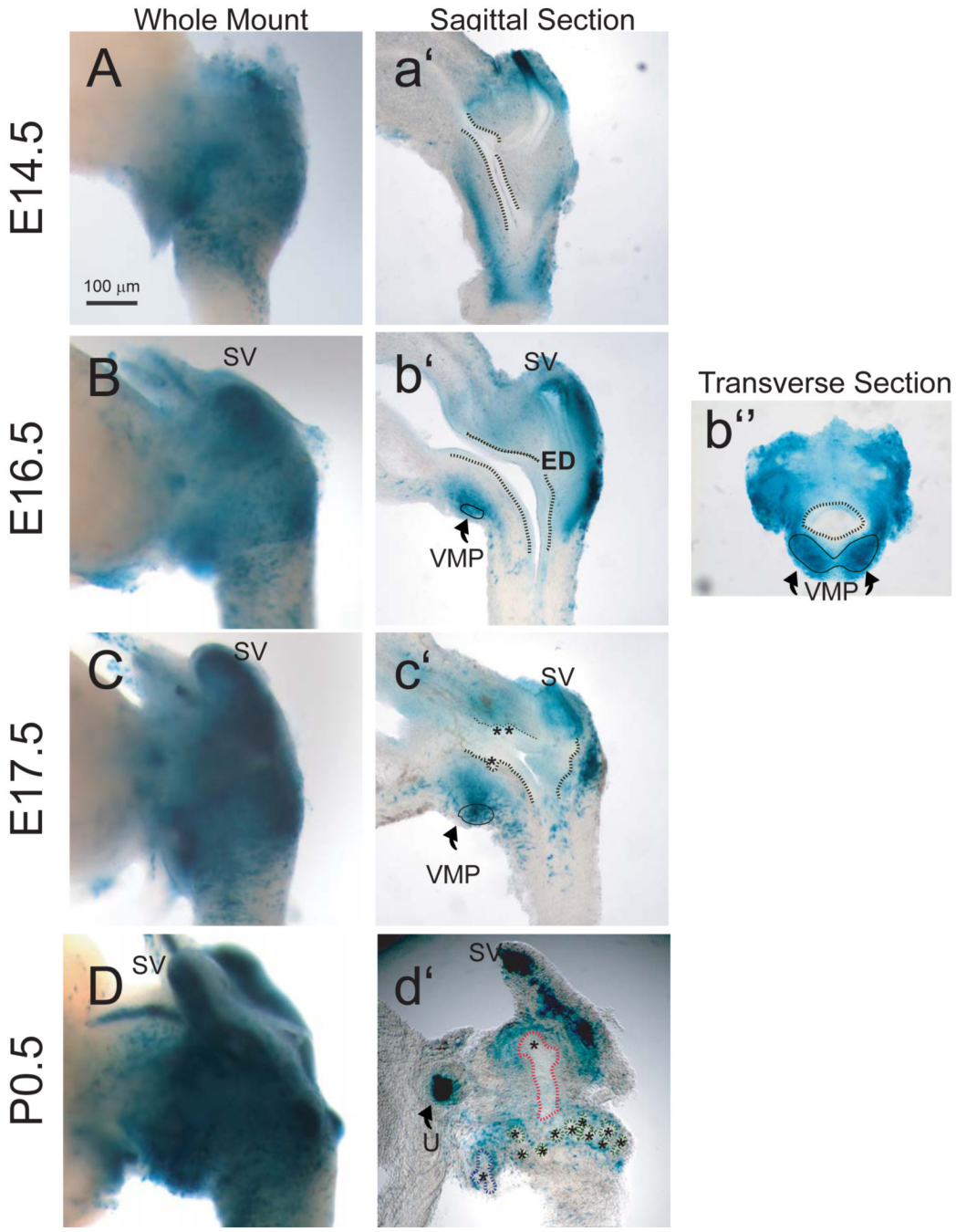

Figure 1. Temporal and spatial expression of retinoid activity in the UGS of male Tg(RARE-Hspa1b/lacZ)12Jrt transgenic mouse fetuses

To assess the temporal expression of retinoid signaling during prostatic budding initiation and elongation, the UGS from fetal male mice that express a *LacZ* transgene under control of a RARE-containing promoter were collected at regular intervals during development from embryonic day (E)14.5 to postnatal day (P)0.5 and probed for β-galactosidase activity. Photographs are representative of $n = 5$ UGS specimens per developmental time point. To evaluate global retinoid activity and activity within specific UGS structures, β-galactosidase activity in UGS specimens was visualized by whole mount imaging (A-D), imaging of sections cut near the mid-sagittal plane (a'-c') or along the sagittal plane near the lateral surface (d'),

and imaging of sections taken along the transverse plane (b”). To enhance visualization, a dotted black line was added to illustrate the boundary between the inner UGS epithelial cell layer and outer mesenchymal cell layer and a solid black line was added to indicate the ventral mesenchymal pad (VMP). Prostatic buds in tissue sections are indicated by asterisks and by colored dotted lines in whole-mount images (blue = ventral buds, green = dorsolateral buds, and red = anterior buds). SV: seminal vesicle; ED: ejactulatory duct; U: ureter.

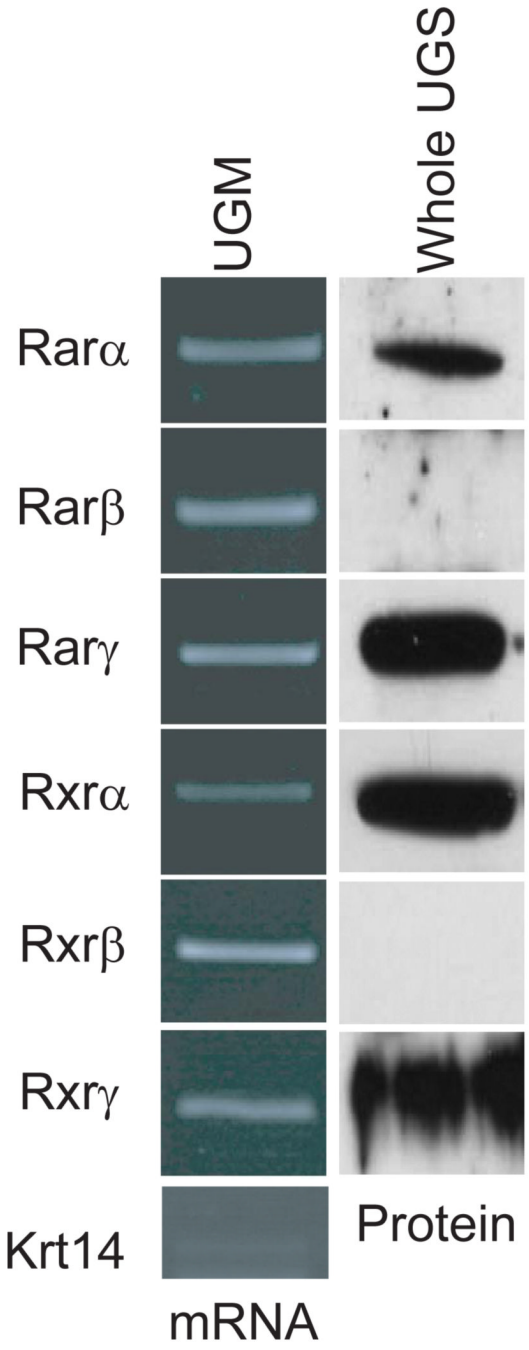

Figure 2. Expression of retinoic acid receptors (RARs) and retinoid x receptors (RXRs) in male mouse UGS

The expression of RARs and RXRs was evaluated at E16.5, during the initiation of prostatic buds from the UGS. Since retinoid activity was most abundant in UGS mesenchyme in Fig. 1, cDNA was synthesized from isolated E16.5 UGS mesenchyme (pooled from $n = 5$ separate fetuses) and purity of this mesenchymal cDNA preparation was demonstrated by showing that it was deficient in the epithelial-specific gene keratin 14 (*Krt14*). All six of the *Rar* and *Rxr* mRNAs were detected in UGS mesenchyme. Immunoblotting was used to determine which RAR and RXR isoforms were present.

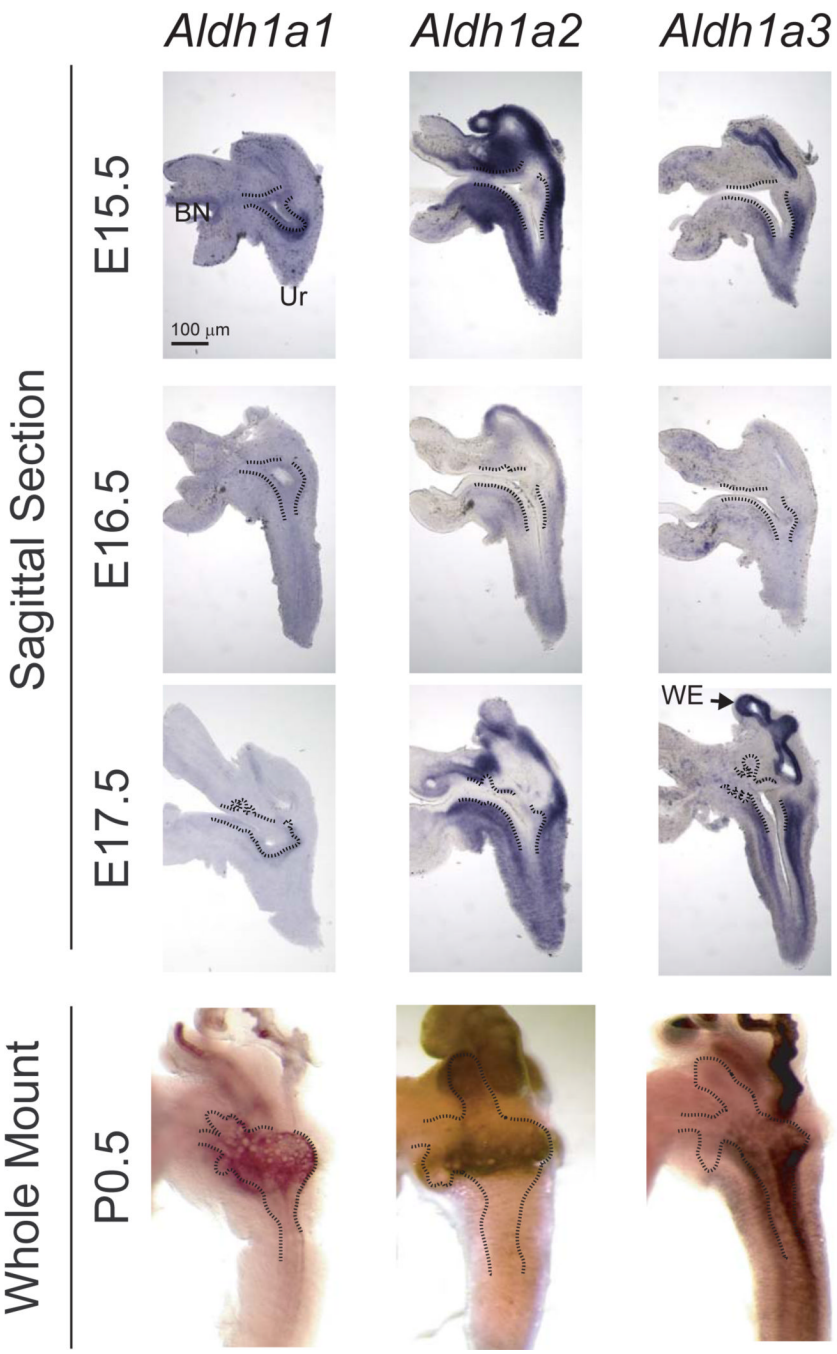

Figure 3. Expression of RA-synthesizing genes in male mouse UGS

The spatial expression pattern of retinaldehyde dehydrogenase (*Aldh*) *1a1*, *1a2* and *1a3* mRNAs was determined in representative E15.5 - 17.5 UGS specimens by ISH on sagittal UGS sections (80 μm) and whole mount UGS and prostate specimens ($n = 5$ UGS and prostate specimens per group). A dotted black line was added to indicate the boundary between the inner layer of UGS epithelium (UGE) and the outer layer of UGS mesenchyme (UGM). Ur: urethra; WE: Wolffian-derived epithelium; BN: bladder neck.

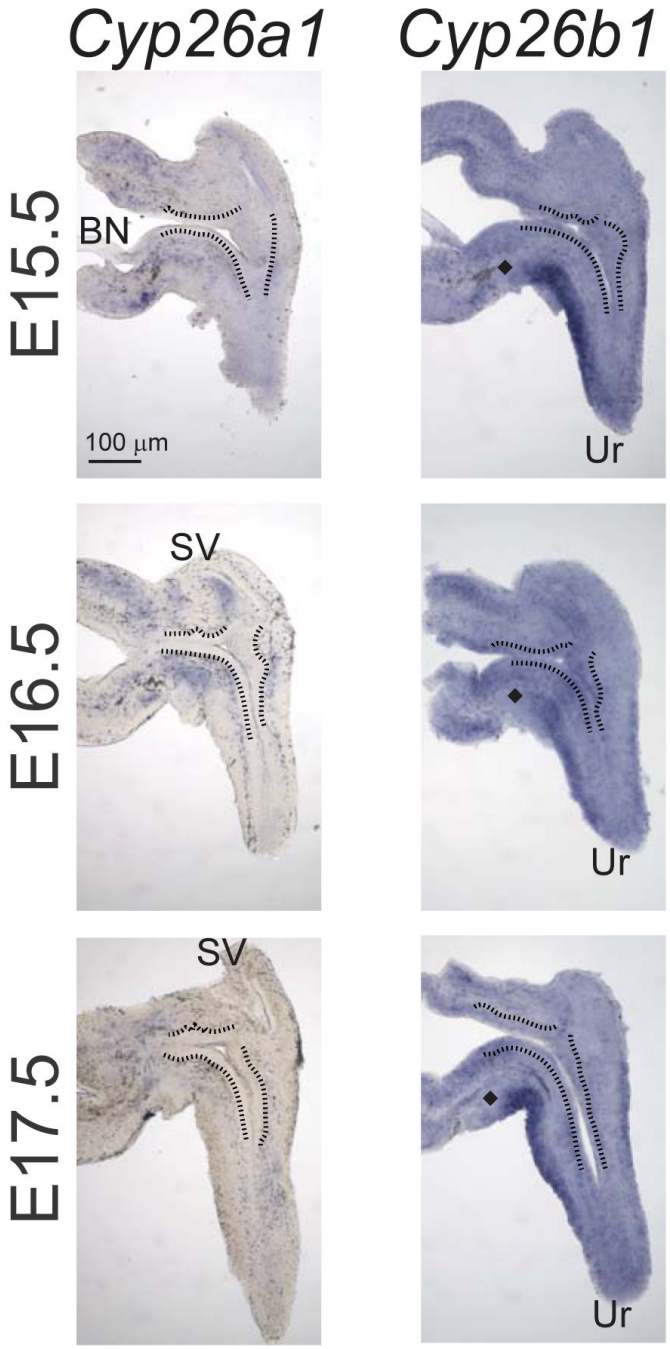

Figure 4. Expression of the RA-metabolizing genes in male mouse UGS

The spatial expression pattern of cytochrome P450 (*Cyp*) *26a1* and *26b1* mRNA was determined in representative E15.5-17 UGS specimens by ISH on 80 μm sagittal UGS sections (n = 3 UGS specimens per group). A black line was added to indicate the boundary between the inner layer of UGE and the outer layer of UGM. At all stages examined between E15.5 - 17.5, there was a gap in *Cyp26b1* expression (indicated by a diamond) proximal to the VMP.

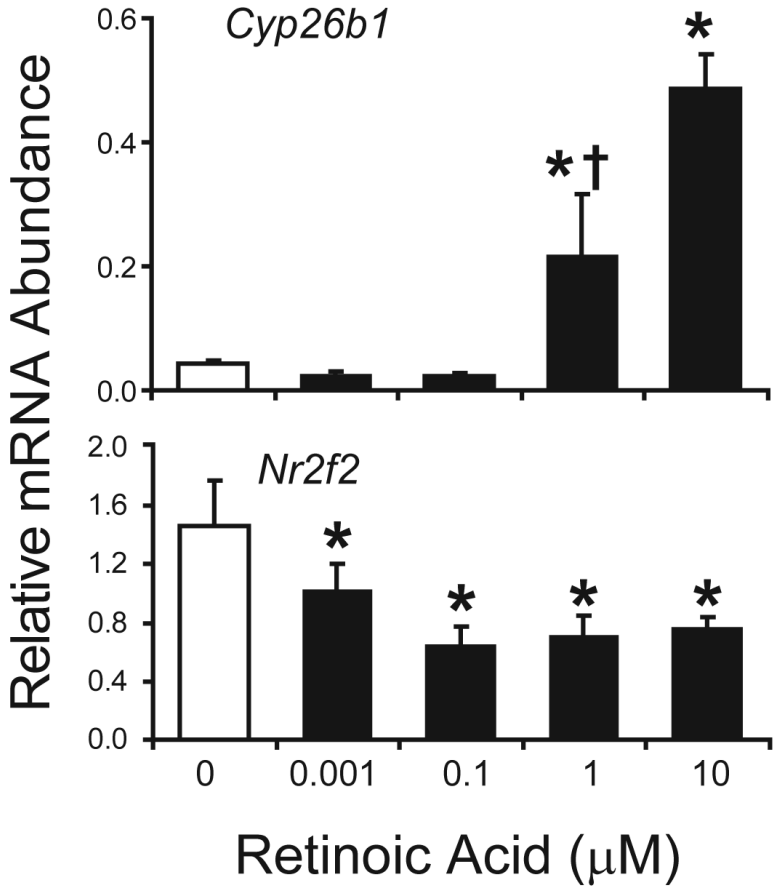

Figure 5. RA induces *Cyp26b1* and represses *Nr2f2* in male mouse UGS organ culture

UGS from E14.5 male C57BL/6J mouse fetuses were incubated for 24 h in organ culture media containing vehicle or RA (0-10 μM). Abundance of *Cyp26b1* and *Nr2f2* was determined by real-time RT-PCR and normalized to the mRNA abundance of the housekeeping gene peptidyl prolyl isomerase a (*Ppia*). Results are mean ± SEM of $n \geq 4$ independent samples per group from at least 3 separate litters. Significant differences among groups were determined by ANOVA followed by Fisher's Least Significant Difference test. The presence of an asterisk indicates significantly different from vehicle (open bars, $p \leq 0.05$). The presence of a dagger indicates significantly different from 10 μM RA ($p \leq 0.05$).

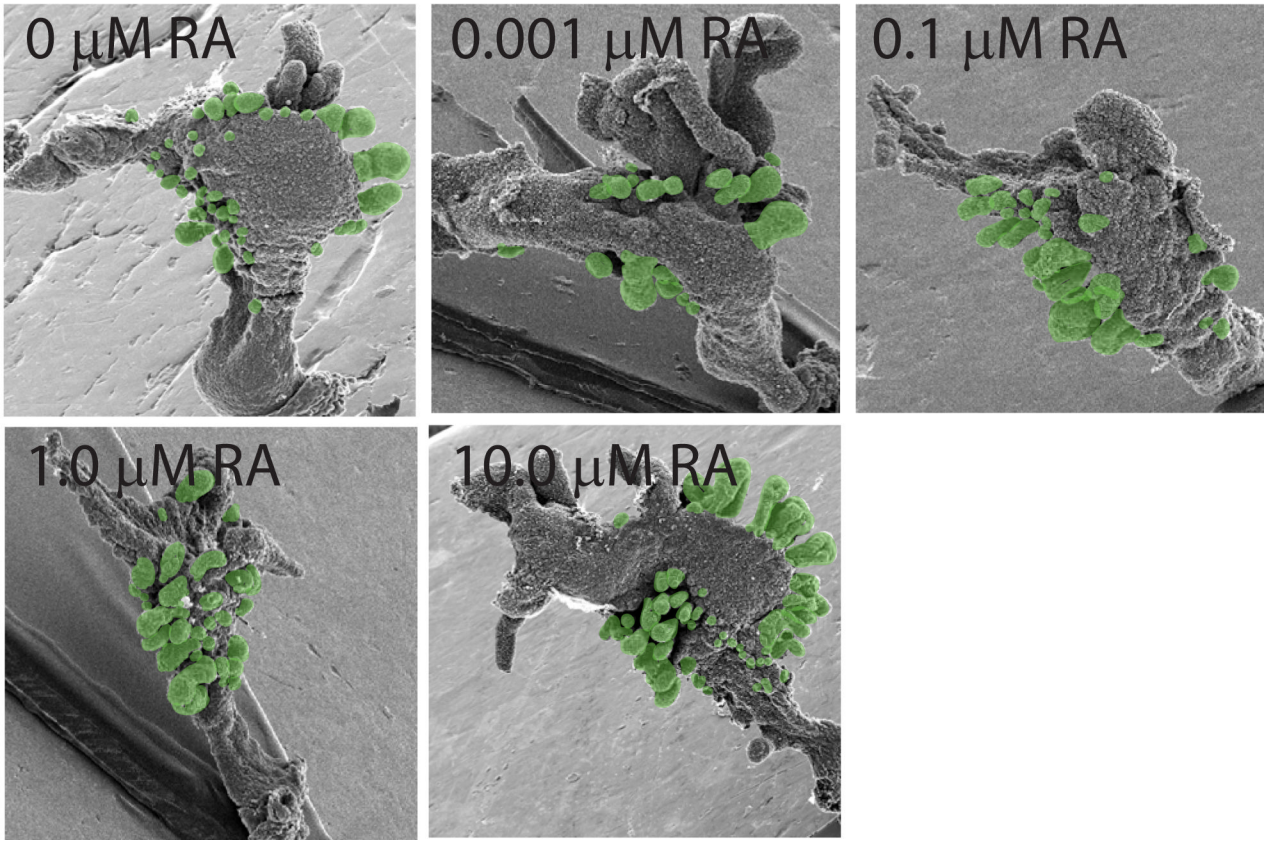

Figure 6. Prostatic bud formation in male mouse UGS organ cultures exposed to RA

UGS from E14.5 male C57BL/6J mouse fetuses were incubated for 3 d in organ culture media containing vehicle or graded concentrations of RA (0-10 μM). Media and RA were replenished after each day. At the end of the incubation, UGE was separated from UGM as described in methods and visualized by SEM. A micrograph representing a single UGE from each exposure group is shown (results are $n \geq 6$ independent samples per group from at least 3 separate litters). Prostatic buds are pseudocolored green.

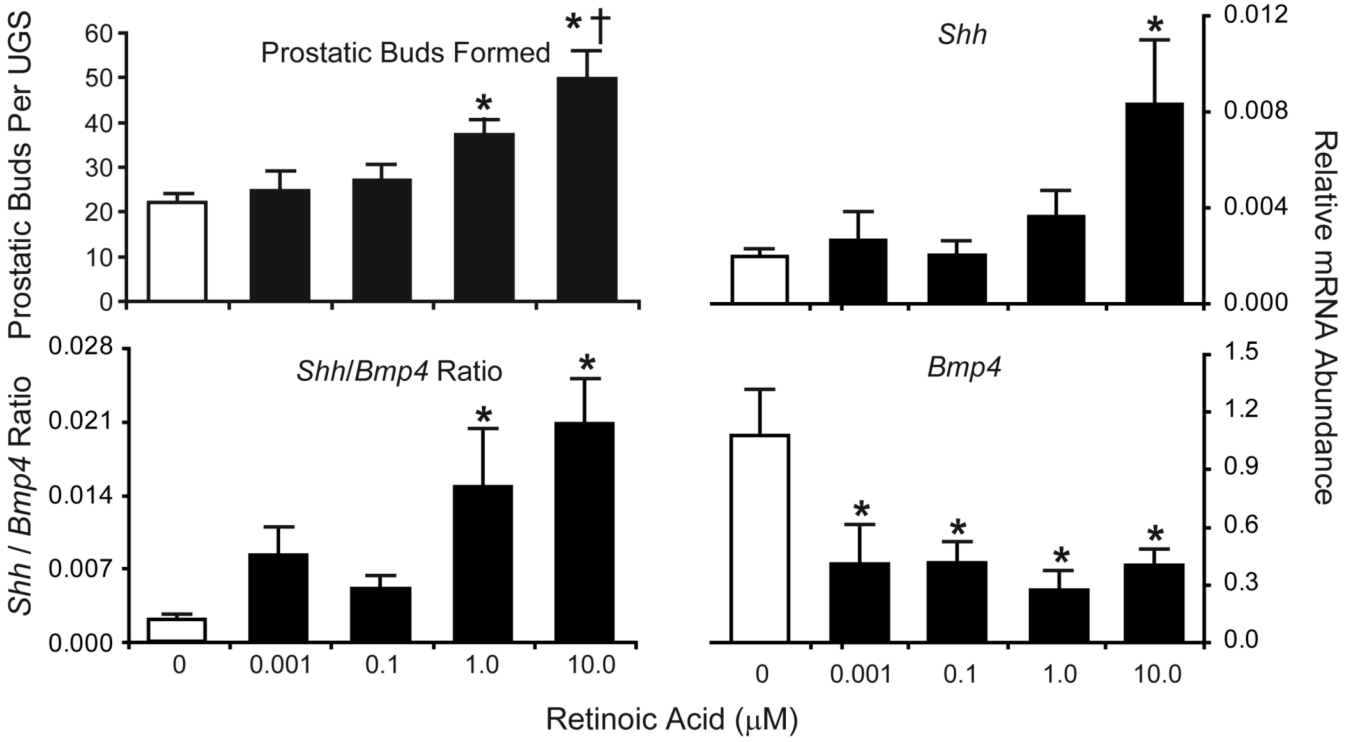

Figure 7. RA induces prostatic bud formation in male mouse UGS organ culture

UGS from E14.5 male C57BL/6J mouse fetuses were incubated for 24 h (for RT-PCR) or 3 d (for prostatic bud counting) in organ culture media containing vehicle or graded concentrations of RA (0-10 μM). Media and RA were replenished after each day. At the end of the 3d incubation, UGE was separated from UGM and visualized by SEM. Prostatic buds were counted using micrographs of each UGS taken from four separate angles in order to observe the entire UGS and ensure that all prostatic buds on the entire UGS epithelial surface were counted. Results for the total number of prostatic buds per UGS are mean ± SEM of $n \geq 6$ independent samples per group from at least 3 separate litters. Abundance of *Shh* and *Bmp4* was determined by real-time RT-PCR and normalized to the mRNA abundance of the housekeeping gene peptidyl prolyl isomerase a (*Ppia*). Results are mean ± SEM of $n \geq 4$ independent samples per group from at least 3 separate litters. Significant differences among means were determined using one-way ANOVA, followed by Fisher's LSD post-hoc test. The presence of an asterisk indicates a mean that is significantly different from the vehicle control (open bars, $p \leq 0.05$). The presence of a dagger indicates it is significantly different from 1 μM RA ($p \leq 0.05$).

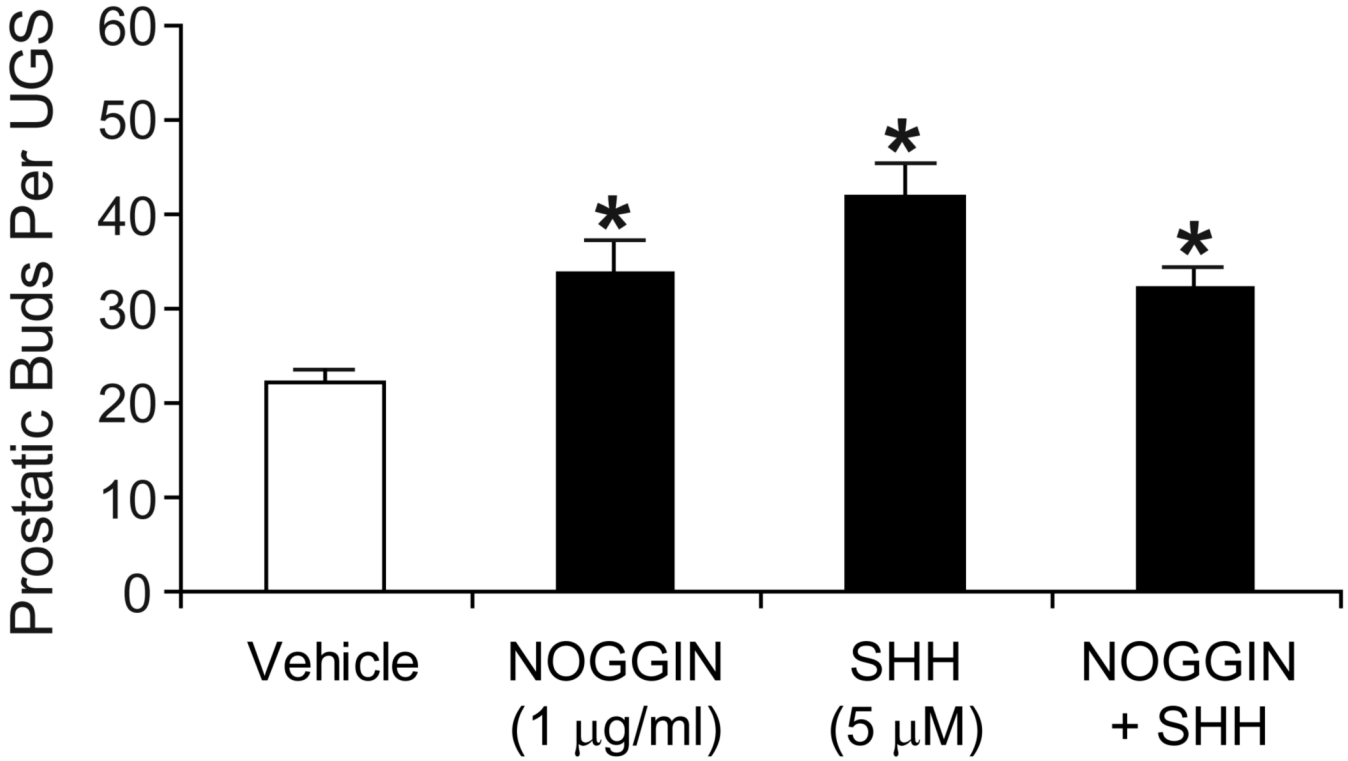

Figure 8. SHH and NOGGIN induce prostatic bud formation in the absence of RA

UGS from E14.5 male C57BL/6J mouse fetuses were incubated for 3 d in organ culture media containing vehicle, recombinant SHH protein (5 μM), recombinant NOGGIN protein (1 ug/ml)or a combination of SHH + NOGGIN. Media and recombinant proteins were replenished daily. At the end of the incubation, UGE was separated from UGM as described in Methods and visualized by SEM. Prostatic buds were counted using micrographs of each UGS that were taken from four separate angles in order to observe the entire UGS epithelial surface and ensure that all prostatic buds present were counted. Results for the total number of prostatic buds per UGS are expressed as the mean ± SEM of $n \geq 6$ independent samples per group for at least 3 separate litters. Significant differences among means were determined using one-way ANOVA, followed by Fisher's LSD post-hoc test. The presence of an asterisk indicates a mean that is significantly different from the vehicle (control) mean ($p \leq 0.05$).